



# Chitin as a universal and sustainable electrode binder for electrochemical capacitors

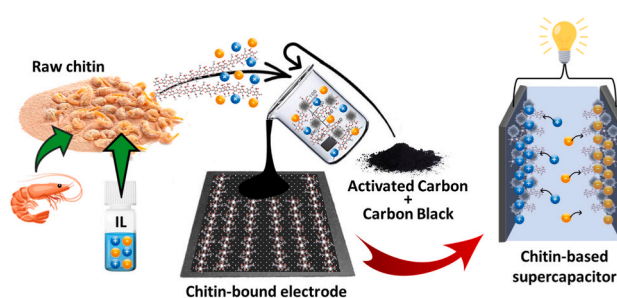
Dawid Kasprzak<sup>\*</sup>, Maciej Galiński

*Institute of Chemistry and Technical Electrochemistry, Poznan University of Technology, Berdychowo 4 St., 60-965, Poznan, Poland*

## HIGHLIGHTS

- Universal and sustainable chitin-bound, AC-based electrode material was designed.
- IL/DMSO mixture solvent was used in the electrode preparation procedure.
- Obtained material exhibited versatility in terms of SC electrolyte compatibility.
- It showed high efficiency in aqueous-, organic-, and ionic liquid-based electrolytes.
- Tested electrodes exhibited  $C_s$  of 128–142 F g<sup>-1</sup> and long-term cycle stability of 75–99%.

## GRAPHICAL ABSTRACT



## ARTICLE INFO

### Keywords:

Biopolymers  
Polysaccharide  
Ionic liquid  
Dimethyl sulfoxide  
Supercapacitor  
Activated carbon

## ABSTRACT

We have introduced chitin-bound, activated carbon-based electrode materials dedicated to supercapacitors operated on different electrolyte environments. As a chitin solvent, we have used our original mixture system containing an ionic liquid (1-ethyl-3-methylimidazolium acetate) and a viscosity reducing agent (dimethyl sulfoxide). The prepared electrode material has been tested in terms of morphological, physicochemical, and electrochemical properties. The most attention has been paid to studying the electrochemical performance of composite electrodes in the most common types of liquid electrolytes, i.e. aqueous, organic and ionic liquid electrolytes. A comparative study of the assembled supercapacitors has been made in terms of specific capacitance, charge propagation, cycle stability, and power/energy density. As was demonstrated, the proposed electrode binder material features a very attractive attribute appearing as versatility in terms of employed electrolyte. Regardless of the type of used electrolyte, chitin-bound electrodes display high specific capacitance (128–142 F g<sup>-1</sup>), good rate capability (up to 92% capacitance retention under 15 A g<sup>-1</sup>), and excellent cycle stability (75–99% of an initial capacitance). Taking into account the natural origin of chitin and the excellent electrochemical efficiency of tested devices, it appears that synthesized electrode materials represent a promising and green alternative for the development of environmentally benign supercapacitors.

## 1. Introduction

The increasing demand for energy-efficient solutions is observed

both in industry and daily life. However, to adapt the energy delivery systems to the global ecological trend, the reduction of fossil fuel consumption and environmental pollution emission is needed. In this

<sup>\*</sup> Corresponding author.

E-mail address: [dawid.kasprzak@put.poznan.pl](mailto:dawid.kasprzak@put.poznan.pl) (D. Kasprzak).

<https://doi.org/10.1016/j.jpowsour.2022.232300>

Received 28 June 2022; Received in revised form 26 September 2022; Accepted 22 October 2022

Available online 31 October 2022

0378-7753/© 2022 The Authors. Published by Elsevier B.V. This is an open access article under the CC BY license (<http://creativecommons.org/licenses/by/4.0/>).

regard, renewable energy resources appear to be one of the most important energy alternatives [1–3]. Unfortunately, the variability of renewable energy is regarded as a challenge for the wide dissemination of renewable technologies. Intermittent renewables are challenging because they are not able to ensure real-time electric demand. Thus, renewable energy technologies require the introduction of efficient energy storage systems to maintain grid stability. The need can be fulfilled by the application of electrochemical energy storage devices. Among many of the investigated technologies, batteries, electrochemical capacitors, and fuel cells are the most important ones, that offer different but often complementary electrochemical properties [4–9].

Crucially, much attention has been recently paid to the development of sustainable and eco-friendly electrochemical energy storage devices [10–12]. Research groups have studied numerous synthesis processes and materials for the realization of policies focused on reduced emission of pollutants and increased contribution of biocompatible and biodegradable components. In the context of supercapacitors, particular efforts have been made for developing and improving the main parts of these devices, electrode materials [13–15] and electrolytes [16–19]. However, the process of supercapacitors transforming into more eco-friendly devices requires also a reconsideration of seemingly insignificant system components. In this context, the electrode material binder is noteworthy. It constitutes a minor part of the electrode construction (usually less than 10 % wt), nevertheless, it is responsible for integrity between the components in the electric network and provides high adhesion to the surface of the current collector [20]. The commonly used fluorinated thermoplastic binders such as polytetrafluoroethylene (PTFE) and poly(vinylidene fluoride) (PVdF) could be the source of possible pollution [21], thus, the eco-friendly, fluorine-free alternatives are in demand. To date, several environmentally benign, water-soluble replacements of fluorine-based polymeric have been provided [21–24], e.g. polyacrylic acid (PAA), polyvinyl alcohol (PVA), carboxymethyl cellulose (CMC), chitosan, alginate, gelatin. Those materials are very easily processed in aqueous media, but this feature excludes their use as electrode binders in systems with aqueous electrolytes. Since supercapacitors based on aqueous ionic conductors display enhanced power performance, this is a pretty restricting feature. To overcome this issue, but retain a sustainable aspect of the electrode, the natural cellulose-based binder [25,26] or reduced graphene oxide (rGO)-based binder for commercial-level mass loading electrodes [27] were proposed. The former material, cellulose, is a biopolymer soluble in some imidazolium-based IL named *green solvents*, but it resists water as well as most organic solvents. Thus, the natural cellulose can act as a universal binder, being stable in all common types of liquid electrolytes dedicated to supercapacitors. We assumed that the same performance can be achieved by the second most abundant biopolymer on the Earth, chitin. Some efforts have been already made to apply chitin as an electrode binder, however, the proposed fabrication process suffers from a lack of sustainability due to the employment of a harsh solvent, *N*-methyl-2-pyrrolidinone (NMP) [28].

Chitin is a polysaccharide widespread in the natural environment [29,30]. Its primary supply is crustacean shell waste, but there are also other materials rich in chitin, including squid pens, some fungi, and fly larvae. The chemical structure of chitin is similar to cellulose. Both biopolymers are composed of several thousand (1–4)- $\beta$ -D-glucose units, but chitin polymeric chains have also acetamide groups instead of hydroxyls at position C-2 of the hexose repeating units [31,32]. Additionally, these polymer chains are arranged in a highly extended hydrogen-bonded structure, causing difficulties associated with chitin solubility in traditional solvents. This feature reflects the industrial application of chitin. Even its attractive properties, such as biocompatibility, biodegradability, mechanical strength, thermal and chemical stability, or favorable biological characteristic, it still remains an unutilized biomass resource on a wide scale [33]. Fortunately, the application of ionic liquids-based solvents looks like a promising step toward the effective and sustainable processing of chitin [19,34–37].

In this study, we have designed universal and sustainable chitin-bound, activated carbon-based electrode materials compatible with the most common types of electrolytes dedicated to supercapacitors. Considering the fact that chitin is hardly soluble in common solvents, we proposed the electrode preparation technique with the chitin solvent comprising imidazolium acetate ionic liquid and dimethyl sulfoxide (DMSO) co-solvent. The designed material stands out from already known biopolymer-based electrode systems, owing to the outstanding electrochemical performance combined with the versatility in terms of electrolyte compatibility. Additionally, the proposed electrode preparation method indicates the sustainable nature due to elimination of harsh solvents. We successfully applied and investigated the chitin-bound electrodes in supercapacitor cells assembled with all common types of liquid electrolytes, i.e. aqueous-, organic-, and ionic liquid-based electrolytes. Besides the electrochemical performance, the morphological and physicochemical characterization of the fabricated chitin-based material was performed. For comparison, analogical activated carbon-based electrodes containing PVdF binder were also considered. For this purpose, the ionic liquid-based solvent has been replaced by *N*-methyl-2-pyrrolidinone (NMP).

## 2. Experimental

### 2.1. Chemicals

$\alpha$ -Chitin extracted from shrimp shells (acetylation degree of 96%) was obtained from BioLog (Germany). Chitin particles were ground to a fine powder by an analytical mill and sieved (the fraction of particles of a diameter smaller than 63  $\mu$ m was used). The powder was dried at 105 °C and not further purified before use. 1-Ethyl-3-methylimidazolium acetate ([EMIm][Ac], purity >95%) was obtained from Iolitech (Germany) and stored under a dry atmosphere in a glovebox chamber (MBraun Plus, Germany). Dimethyl sulfoxide (P.O. Ch. Poland) was used as received. Electrode materials were prepared using activated carbon AC (powder; Norit DLC Supra 30) as an active material, acetylene carbon black CB (Alfa Aesar; 50% compressed) as a conductive agent, and woven carbon cloth (W1S1010, CeTech, China; 410  $\mu$ m) as a current collector. Chitin was used as investigated electrode binder. However, we also used poly(vinylidene fluoride) (PVdF) powder (Sigma-Aldrich) and *N*-methyl-pyrrolidone (NMP) (Sigma-Aldrich) for the preparation of electrodes with the reference fluorinated binder.

As electrolytes, we employed 1 M lithium sulphate  $\text{Li}_2\text{SO}_4$  (monohydrate, BioUltra,  $\geq 99.0\%$ ) aqueous solution, 1 M tetraethylammonium tetrafluoroborate  $\text{Et}_4\text{NBF}_4$  (purity  $\geq 99\%$ , Sigma-Aldrich) organic solution in propylene carbonate (Sigma-Aldrich), and neat ionic liquids, 1-ethyl-3-methylimidazolium tetrafluoroborate [EMIm][BF<sub>4</sub>] (Iolitech, purity 99%) and *N*-methyl-*N*-propylpyrrolidinium bis(trifluoromethylsulfonyl)imide [MPPyr][TFSI] (Iolitech, purity 99.5%). A glass microfiber filter (GF/A, Whatman) was used as a separator material.

### 2.2. Preparation of chitin-bound carbon electrodes

The chitin-bound electrode material was prepared by the slurry casting technique. The schema of the electrode preparation was presented in Fig. 1. Prior to the slurry preparation, the chitin solution was obtained. For this purpose, we used our already reported procedure of chitin processing in the ionic liquid solvent with the assistance of a dimethyl sulfoxide (DMSO) co-solvent [38]. The task of DMSO is the reduction of solution viscosity, which facilitates the operations on solubilized chitin.

First, 15 mg of chitin powder was placed into a glass vial containing 0.5 g of [EMIm][Ac]. Then, the system was mixed with a magnetic stirrer and heated to 120 °C until the homogeneous, pale yellow, and the very viscous solution was obtained. Further, 1.5 g of DMSO was added to the chitin solution, followed by the stirring homogenization at 120 °C.

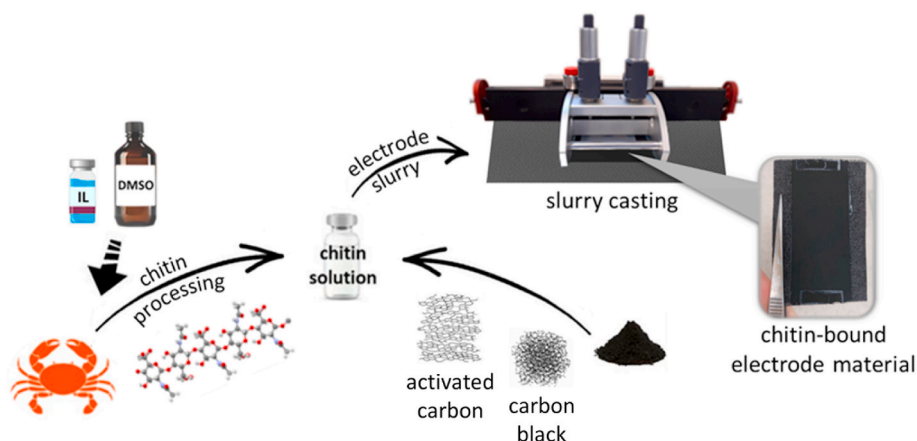


Fig. 1. The schema of chitin-bound electrode preparation.

Finally, the obtained clear solution was mixed with a dry mixture of activated carbon (270 mg) and carbon black (15 mg). The whole system was homogenized by a magnetic stirrer with constant heating at 120 °C for ca. 30 min.

Previously obtained black slurry mixture was hot-cast on woven carbon cloth current collector using doctor blade film applicator. The surface of the application table was heated at 80 °C during the casting procedure. The electrode slurry was cast on the surface of the current collector using a casting knife with a casting thickness of 200 μm. Subsequently, the chitin-bound electrode material was left on the heated casting table for 30 min for pre-drying (DMSO evaporation). Then, the coated electrode was immersed in deionized water in order to remove IL from the surface of this material. After 24 h and several additional washes, the chitin-bound electrode material was transferred into a laboratory dryer and left for overnight drying at 120 °C, followed by additional vacuum drying at 80 °C for 24 h. Finally, the electrodes were cut out into 11.8 mm diameter discs for further tests. The average mass of the single electrode (without current collector mass) was 3 mg. The mass loading of the active material was ca. 2.5 mg cm<sup>-2</sup>.

For comparison, the activated carbon-based electrodes with the same composition, but containing PVdF binder were also synthesized. The binder solution was prepared by dissolving PVdF in *N*-methyl-2-pyrrolidinone. Because of the difference in the coagulation procedure, deionized water was not used during the fabrication of PVdF-based electrode material. The rest conditions of the preparation procedure remained unchanged.

### 2.3. Characterization techniques

The morphology of chitin-bound electrode material was investigated by scanning electron microscopy (SEM). SEM images were taken using the Hitachi S-3400 N scanning electron microscope. The energy dispersive spectroscopy (EDS) technique was used for the qualitative analysis of the investigated materials.

The nitrogen adsorption-desorption isotherms were investigated at 77 K using the ASAP 2010 (Micromeritics Instrument Corporation, USA) sorptometer. On the grounds of the results, a specific surface area (SSA) of tested samples was calculated by the Brunauer-Emmett-Teller (BET) method. Additionally, the pore size distribution (PSD) was estimated from the adsorption branches of isotherms using the Barrett-Joyner-Halenda (BJH) method.

Thermogravimetric measurements were carried out using a thermal gravimetric analyzer (TG 209 Libra, Netzsch, Germany). For each sample, the temperature was scanned from 25 to 600 °C at a fixed heated rate of 10 °C min<sup>-1</sup>. All experiments were performed under a nitrogen purge at a flow rate of 20 ml min<sup>-1</sup>.

The ionic conductivity of the investigated electrolytes was performed

by the electrochemical impedance spectroscopy (EIS) technique using the Interface 5000 device (Gamry Instruments, USA). The measurements were carried out using the conductivity cell with two parallel and symmetrical platinum electrodes at a constant temperature of 25 °C. The electric conductivity of the current collector and chitin-bound electrode material was estimated using a four-point probe technique. The values of their thickness were measured using a digital coating thickness gauge (PosiTector 6000, DeFelsko, USA).

The chitin-bound electrode material was electrochemically tested in Swagelok®-type cells assembled with several different electrolytes: 1 M Li<sub>2</sub>SO<sub>4</sub> aqueous solution, 1 M Et<sub>4</sub>NBF<sub>4</sub> organic solution in propylene carbonate, neat [EMIm][BF<sub>4</sub>] hydrophilic ionic liquid, and neat [MPPyrr][TFSI] hydrophobic ionic liquid. Except for the aqueous-based system, all supercapacitors were assembled in a glove-box chamber under the inert atmosphere (Ar, H<sub>2</sub>O < 0.5 ppm; O<sub>2</sub> < 0.5 ppm; MBraun Plus, Germany). The three-electrode Swagelok® compartments were applied, allowing both two- and three-electrode measurements. The pseudoreference electrodes made of silver wires covered electrochemically with silver chloride (Ag|AgCl) were used. In each testing cell, the reference electrode was placed in the space (filled with electrolyte) between two symmetric chitin-bound electrodes of the capacitor, to enable control of potential changes of oppositely charged electrodes, separately.

The electrochemical performance of assembled capacitors was investigated by commonly known electrochemical techniques, such as cyclic voltammetry (CV), electrochemical impedance spectroscopy (EIS), and cyclic galvanostatic charge-discharge (GCD). All of these measurements were performed on a multi-channel potentiostat/galvanostat Interface 5000 device (Gamry Instruments, USA). Potentiodynamic analysis was taken at sweep rates from 5 to 100 mV s<sup>-1</sup>, and galvanostatic cycling was carried out at constant current densities in the range of 0.1–15.0 A g<sup>-1</sup>. All these tests were conducted in the voltage range specified for each type of the applied electrolyte at ambient conditions. Specifically, 0–0.9 V for the aqueous-based system, 0–2.7 V for the organic-based system, 0–3.0 V for the EMImBF<sub>4</sub>-based system, and 0–3.5 V for the MPPyrrTFSI-based system. The maximum voltage was chosen according to the preliminary study. EIS measurements were carried out applying a potential amplitude of 10 mV and a frequency range from 0.01 Hz to 100 kHz at ambient conditions.

The specific capacitances of investigated systems were calculated according to the equation

$$C = \frac{2 \int Idt}{\Delta V \cdot m_E} \quad (1)$$

in the case of cyclic voltammetry measurements and

$$C = \frac{2I}{(\Delta V / \Delta t) \cdot m_E} \quad (2)$$

in the case of cyclic charge-discharge measurements, where  $I$  is current,  $\Delta V$  is maximum working voltage,  $\int Idt$  is the area under the CV curve (cathodic scan),  $\Delta V / \Delta t$  is the slope of potential change during discharge, and  $m_E$  is the mass of the individual electrode.

The important parameters of every electrochemical storage device are energy and power density. In the case of a supercapacitor, the maximum energy density ( $E$ ) can be calculated using the equation:

$$E = \frac{CU^2}{2} \quad (3)$$

where  $C$  is the specific capacitance of the supercapacitor and  $U$  is the operating voltage.

The maximum power density ( $P$ ) may be calculated as

$$P = \frac{E}{t_d} \quad (4)$$

where  $t_d$  is the discharge time recorded in the GCD experiment.

For all the tested capacitors, the energy and power density were calculated per mass unit of the whole electrode material of the device.

### 3. Results and discussion

The morphology of synthesized chitin-bound electrode materials was estimated by SEM analysis. In Fig. 2, there are several SEM images presenting the surface of the neat current collector and chitin-bound electrode material. As can be seen, a flat and microporous surface of the woven carbon cloth current collector was successfully covered by a uniform layer (thickness of ca. 100  $\mu\text{m}$ ) containing a mixture of activated carbon and carbon black particles integrated by the chitin binder. The nano-sized carbon black particles are homogeneously distributed around relatively large AC particles, creating a well-packed electrical network stabilized by the chitin matrix. No sign of agglomeration and long-distance cracking was observed either. Generally, the morphological structure of the chitin-bound electrode is very similar to the cellulose-bound carbon electrode investigated by our research group in the previous paper [26]. The electronic conductivity measurements of the chitin-based electrode seem to confirm a well-harmonized distribution of active material on the surface of the current collector. In fact, the thin electrode layer bound by biopolymer that featured insulating

properties has decreased the electrical conductivity of the whole electrode material compared to the neat current collector. However, the difference is not significant and the chitin-bound composite electrode displayed a high electrical conductivity of 45.15  $\text{S cm}^{-1}$ , compared to 50.98  $\text{S cm}^{-1}$  estimated for the neat woven carbon cloth current collector, as measured by a four-point probe method. It suggests that chitin could be successfully applied as an electrode binder, which will be also proved by further electrochemical tests discussed in this paper.

Additionally, the SEM post mortem analysis of the aged chitin-based electrodes after long-term GCD cycling (10,000 at 1  $\text{A g}^{-1}$ ) in different electrolyte environments was introduced in Fig. S1. As can be seen, the surfaces of the investigated electrodes, regardless of the type of used electrolyte, are barely changed during the cyclic ageing tests. When comparing the SEM images taken for these materials to the morphology of the fresh electrode surface presented in Fig. 2b, no substantial differences can be noticed. It suggests good mechanical properties and excellent electrochemical stability of the designed chitin-bound electrode material.

Nitrogen adsorption-desorption isotherm analysis was applied to reveal the influence of individual components on the porous character of the whole investigated chitin-bound electrode material. Fig. 3a presents nitrogen sorption isotherm recorded for the individual components of the chitin-based electrode (also activated carbon:carbon black dry mixture) treated as reference samples and final chitin-bound electrode material (without current collector). As can be seen, the tested composite electrode, as well as all activated carbon-based samples, they all displayed type I, pseudo-Langmuir BET isotherm profile [39,40]. In all cases, a significantly enhanced nitrogen adsorption occurred at a low relative pressure (below 0.1  $P/P_0$ ), suggesting a predominant microporosity structure of those materials. In contrast, the carbon black sample exhibited a typical type IV BET isotherm profile with a hysteresis loop, indicating the presence of a mesoporous structure [41]. Finally, as was expected, inactive chitin film showed a very low adsorption quantity in the whole relative pressure range, indicating poor porosity structure. The volume of absorbed nitrogen is the highest for the pure activated carbon sample and it becomes lower in the case of AC/CB mixture sample and manufactured chitin-bound electrode material due to the presence of additives with low surface area, i.e. carbon black and/or chitin. The BET surface area of neat activated carbon was ca. 1860  $\text{m}^2\text{g}^{-1}$ , while the investigated chitin-bound electrode material displayed ca. 1300  $\text{m}^2\text{g}^{-1}$ . Table 1 summarized the results of estimating BET surface area for all tested samples.

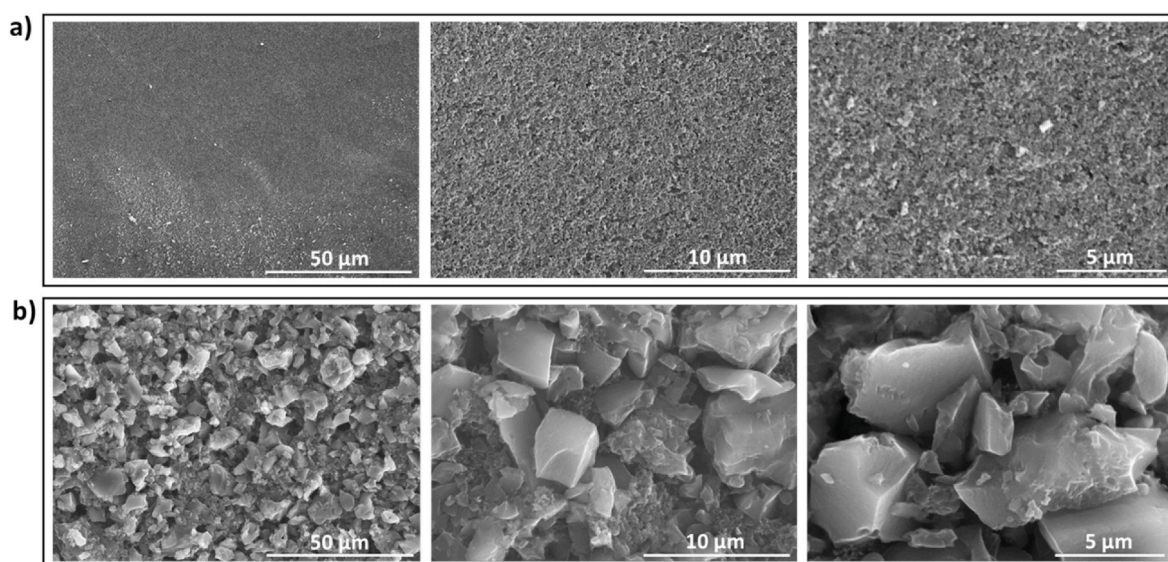


Fig. 2. SEM morphology study of the current collector (a) and chitin-bound electrode (b).

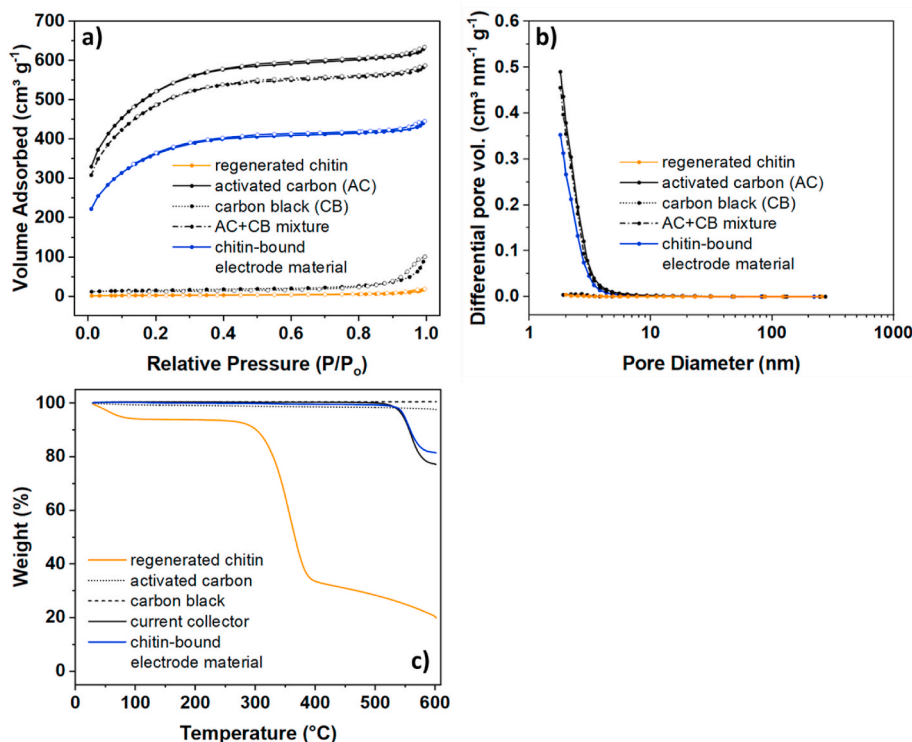


Fig. 3. Nitrogen sorption isotherms (a), pore size distribution curves (b), and thermogravimetric analysis (c) of the chitin-bound electrode material and reference samples.

Table 1

The summary of BET specific surface area and pore volume values for chitin-bound electrode material and reference samples.

Sample	BET Surface Area m <sup>2</sup> g <sup>-1</sup>	Cumulative Pore Volume cm <sup>3</sup> g <sup>-1</sup>
activated carbon (AC)	1858	0.46
carbon black (CB)	50	0.15
AC + CB mixture	1732	0.41
regenerated chitin	8	0.03
chitin-bound electrode material	1298	0.33

Pore size distribution (PSD) curves obtained from the adsorption branches of isotherms using the BJH method are shown in Fig. 3b. The PSD curves show that activated carbon-based samples possess micropores and mesopores, indicating that the micropore feature is dominated [42]. These results are in accordance with the sorption isotherm analysis discussed above. The calculated total pore volumes for activated carbon, activated carbon:carbon black mixture, and chitin-bound electrode material were 0.46 cm<sup>3</sup>g<sup>-1</sup>, 0.41 cm<sup>3</sup>g<sup>-1</sup>, and 0.33 cm<sup>3</sup>g<sup>-1</sup>, respectively. The results confirm our expectations and previous observation. The addition of nonactive additives reduces the free access to the pores of electrode material. The decreased pore volume is mainly caused by the biopolymeric binder, which partly collapses the porous structure of activated carbon. Nevertheless, the reduction of the specific surface area is not so dramatic, and importantly, it is a necessary compromise between the highest active surface area and the mechanical stability between particles and the current collector.

The thermal stability of chitin-bound electrode material was investigated by thermogravimetric analysis. This time, the electrode material was analyzed along with the current collector. Besides the final product, its constituent components were also tested as separate ones, reference samples. As can be seen in Fig. 3c, the thermal stability of the chitin-bound electrode is limited by the chitin binder. Regenerated chitin foil loses the major of its weight above ca. 300 °C, whereas the rest of the

analyzed components are thermally stable until at least 500 °C. Obviously, it doesn't mean that chitin is an inappropriate electrode component. The estimated thermal stability of chitin is very high and completely sufficient in terms of application in electrochemical storage devices. The other electrode components, activated carbon and carbon black, lost only a few percent of their initial weight during the TGA measurement with the same temperature range. The current collector, however, has thermally decomposed above 500 °C, losing about 25% of its initial mass. Because the greatest share in weight of electrode material held current collector, the TGA profile of chitin-bound electrode is similar to that recorded for the current collector. However, as was said before, the investigated chitin-bound electrode material could be thermally stable below the decomposition temperatures of the chitin binder, i.e. ca. 300 °C.

Fig. 4 presents the cyclic voltammetry performance of symmetric supercapacitors in 2-electrode system, containing synthesized chitin-bound electrode material and several different liquid electrolytes mentioned in the **experimental section**. As can be seen, all tested devices exhibited excellent electrochemical performance with the maximum operating voltage typical for the applied electrolyte. In all cases, the shape of CV profiles displays box-type characteristics with excellent charge propagation, even at relatively fast scan rates. It indicates that all tested electrolytes have well wetted the surfaces of the investigated electrodes and the charge propagation easy correlate with the conductivity of the applied electrolytes (Table S1). In fact, the system with an aqueous electrolyte predominates in terms of charge propagation, ahead of the ones that applied an organic electrolyte and ionic liquid-based electrolytes, respectively. Naturally, the deviations from a rectangular shape of CV curves increase with the increasing scan rate, however, it is a typical capacitive phenomenon, limited by the kinetic of electric double layer formation. The small distortions from purely capacitive behaviour could be observed for systems containing ionic liquid-based electrolytes (Fig. 4c–d), but those are not obvious shreds of evidence for the decomposition of the electrode or the electrolyte. We presumed that these minor peaks come from the residual

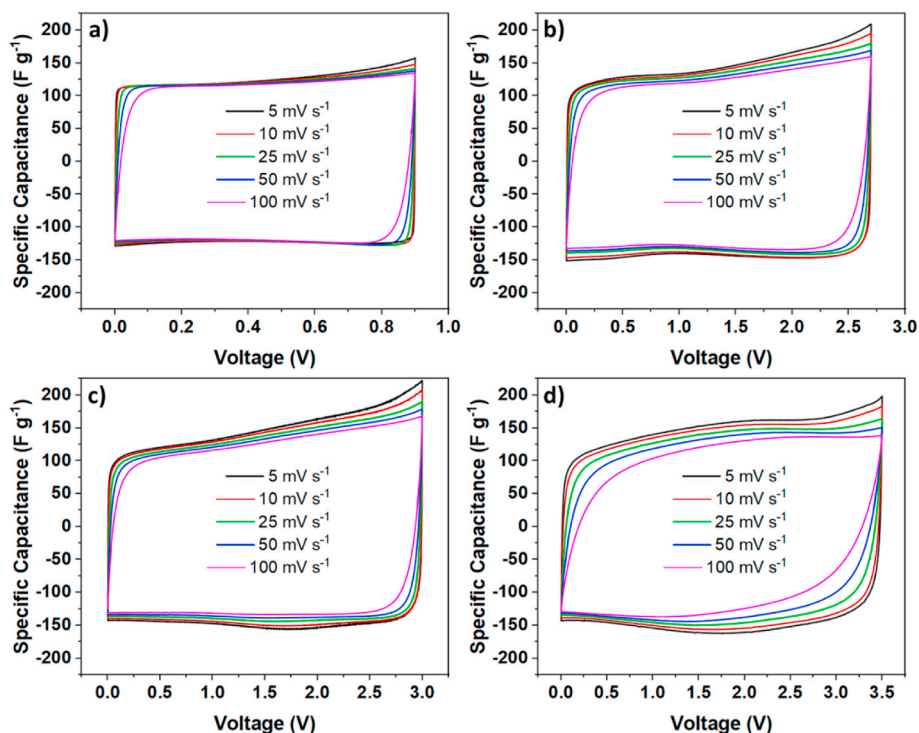


Fig. 4. Cyclic voltammograms of supercapacitors containing chitin-bound electrodes and 1 M  $\text{Li}_2\text{SO}_4$  aqueous electrolyte (a), 1 M  $\text{Et}_4\text{NBF}_4$  organic electrolyte (b),  $[\text{EMIm}][\text{BF}_4]$ -based electrolyte (c), or  $[\text{MPPyrr}][\text{TFSI}]$ -based electrolyte (d).

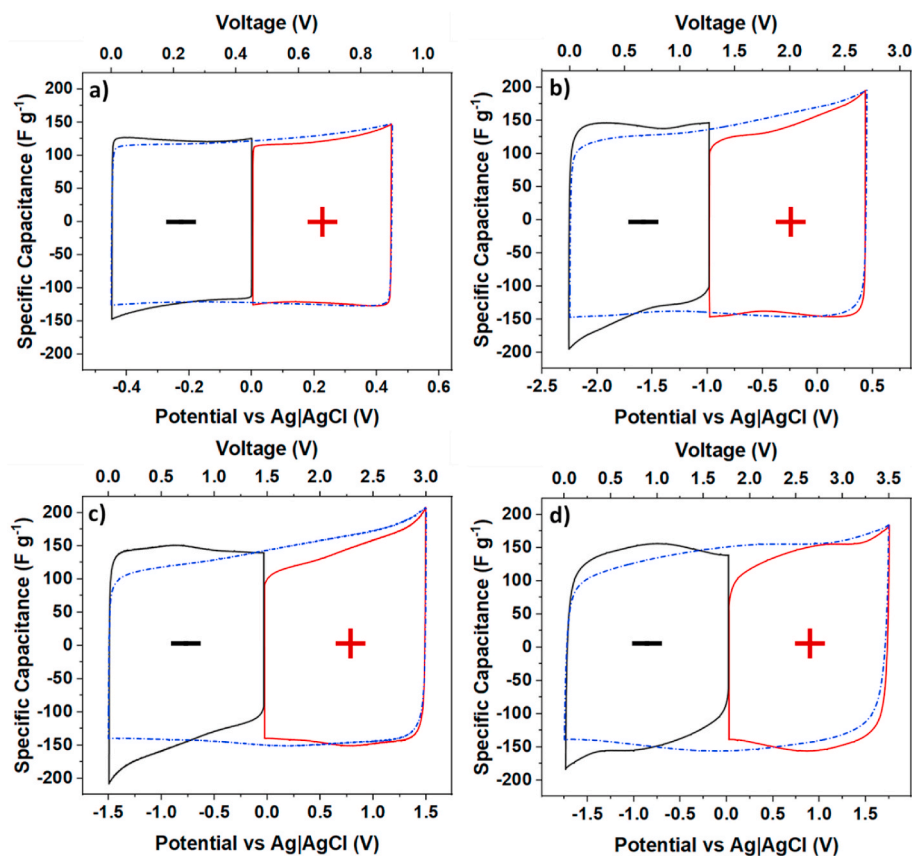


Fig. 5. Cyclic voltammograms in three-electrode system recorded for supercapacitors containing chitin-bound electrodes and 1 M  $\text{Li}_2\text{SO}_4$  aqueous electrolyte (a), 1 M  $\text{Et}_4\text{NBF}_4$  organic electrolyte (b),  $[\text{EMIm}][\text{BF}_4]$ -based electrolyte (c), or  $[\text{MPPyrr}][\text{TFSI}]$ -based electrolyte (d). Voltammograms were recorded at  $10 \text{ mV s}^{-1}$  (vs. counter electrode).

moisture in the biopolymer binder (Fig. 3c, regenerated chitin). However, as will be discussed later, the long-term electrochemical investigation of chitin-bound electrode material led to the assumption that mentioned CV distortions do not reflect the ageing effect of supercapacitors.

The reference electrode material with PVdF binder has not shown such a universality (in terms of applied electrolyte) as the chitin-bound electrodes (Fig. S2). Compared to investigated material, the reference electrode exhibited worse charge propagation and decreased electrochemical stability, observed as a significant current rise near the value of maximum working voltage.

In order to evaluate the electrochemical performance of both chitin-bound electrodes of each device separately, the three-electrode measurements were additionally carried out on supercapacitors assembled with the pseudoreference electrodes. In Fig. 5, the cyclic voltammograms recorded at  $10 \text{ mV s}^{-1}$  (whole cell) for devices that applied each type of investigated electrolyte were presented. As can be seen, CV profiles for both electrodes of each tested supercapacitor show the highly symmetric characteristic for the 3-electrode regime. The voltammograms display purely capacitive shapes without remarkable deviations in a form of redox peaks. It could only be mentioned here that the existence of small *humps* is observed during the inspection of CV profiles recorded for capacitors assembled with ionic liquid-based electrolytes. This observation corresponds with insights made based on 2-electrode monitoring measurements. However, as was mentioned before, these minor pseudo-capacitance effects do not significantly affect the lifespan of investigated chitin-bound electrode-based supercapacitors.

The electrochemical impedance spectroscopy technique was incorporated to estimate the internal resistance properties of supercapacitors assembled with chitin-bound electrode material and various model liquid electrolytes. Fig. 6 shows Nyquist plots recorded for all tested devices (the fitted Nyquist plots along with equivalent circuits applied for the fitting calculations are provided in Fig. S3). As can be seen, the impedance spectrum for each studied supercapacitor is shifted towards the lower impedance values and indicates a typical capacitive behaviour with a straight line in the low-frequency region. However, the type of applied electrolyte determined the exact shape of the EIS profile. It could be correlated with the conductivity performance of each analyzed electrolyte. Therefore, the EIS spectrum of the aqueous-based device seems to be most similar to the ideal model system, but the change of the

electrolyte to organic- and ionic liquid-based, respectively, causes the impairment of the impedance performance, e.g. shifting towards higher impedance values, increasing of the EIS curve slope angle, or appearing of diffusion-limiting part of the spectrum in medium-frequency region. Even though the EIS results differ between analyzed systems, the presented characteristics generally are very good for all devices. It only confirms the versatility of chitin-bound electrode material as a working component in various electrolyte mediums. Table 2 shows impedance parameters calculated from EIS spectra. It provides a numerical summary of our above discussion. Additionally, the data for reference systems (employing PVdF-based electrodes) was presented in this table. Comparing experimental values and the shapes of EIS profiles (for PVdF-based systems – see Fig. S4), it seems that the chitin binder exhibited better electrolyte versatility and high compatibility with the applied carbon cloth current collector.

Apart from voltammetry and impedance studies, the behaviour of chitin-bound electrodes was also investigated using galvanostatic charge and discharge measurements. Fig. 7 presents initial GCD profiles for devices assembled with several different electrolytes, in both two- and three-electrode systems at  $1 \text{ A g}^{-1}$  current density. The typical triangular shape of the GCD curves with a negligible potential drop for all the investigated devices is observed. Here, the same as for previous measurements, the relationship between the internal resistance of the device and the type of applied electrolyte is observed. The ohmic drop recorded for the system with the aqueous electrolyte is almost unnoticeable, while it becomes considerable for the MPPyrrTFSI-based cell. The capacitive and symmetric behaviour of chitin-bound electrodes was additionally observed by analysing three-electrode results. The recorded curves indicate no remarkable faradaic contribution to the charge accumulation on both electrodes for each capacitor.

The reference systems with PVdF electrode binder displayed very similar GCD characteristics (Fig. S5), however, the capacitor systems containing the hydrophilic type of electrolytes (aqueous  $\text{Li}_2\text{SO}_4$  and EMImBF<sub>4</sub>) again stand out noticeably from the rest devices. The charging profiles for those systems exhibited distorted linear shapes, caused by high series resistance. This phenomenon in conjunction with semicircles observed on the impedance spectra (Fig. S4) or exponential increases in current response at high polarization during CV measurements (Fig. S2), suggests ion diffusion limitations or parasitic side reactions because of overcharge. Since PVdF is commonly used as a binder for electrode materials, we assumed that the lack of its performance comes from insufficient adhesion to the surface of the applied current collector. As a summary, Table 3 contains capacitance values calculated for chitin- and PVdF-bound electrode materials from CV and GCD measurements.

Fig. 8a–b shows the investigation of the electrode rate capability, presented as capacitance retention dependencies of CV scan rate and discharging current density, respectively. For all investigated systems, chitin-bound electrodes display excellent capacitance retention. Their high performance at the increasing scan rate is reflected as at least 75% capacitance retention. Similarly, the capacitance efficiency at the increasing current loads is very satisfying, reaching for tested devices up to 92% capacitance retention under  $15 \text{ A g}^{-1}$  current density. The lowest power performance was exhibited by the MPPyrrTFSI-based system, however, this device led in terms of energy density, which will be discussed later in the text. For comparison, the results for analogical

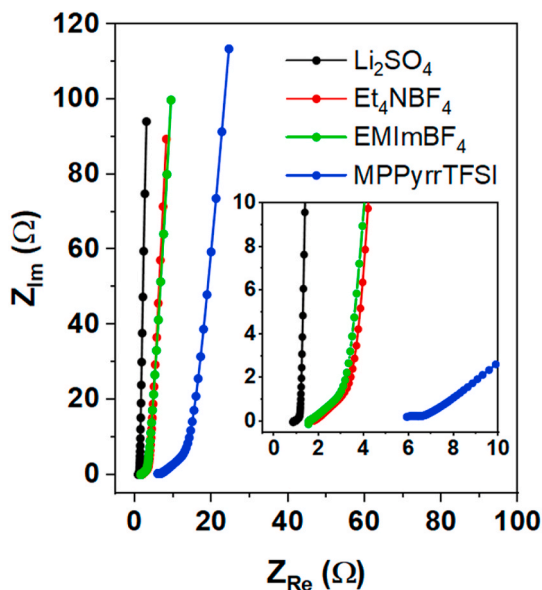


Fig. 6. Electrochemical impedance analysis of supercapacitors assembled with chitin-bound electrodes and various liquid electrolytes.

Table 2  
The summary of electrochemical impedance spectroscopy analysis.

Electrolyte	chitin-based binder		PVdF-based binder	
	ESR [ $\Omega$ ]	EDR [ $\Omega$ ]	ESR [ $\Omega$ ]	EDR [ $\Omega$ ]
1 M $\text{Li}_2\text{SO}_4$ in $\text{H}_2\text{O}$	0.9	1.2	2.8	4.9
1 M TEABF <sub>4</sub> in PC	1.7	3.7	2.5	3.9
EMImBF <sub>4</sub>	1.5	3.4	2.6	6.1
MPPyrrTFSI	6.1	13.8	5.8	12.1

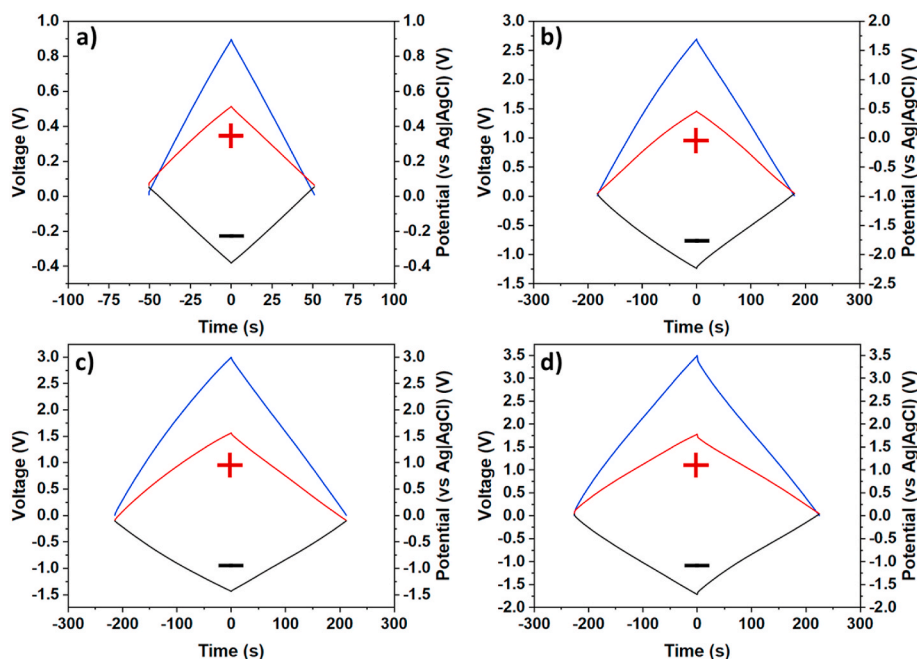


Fig. 7. Electrochemical performance of supercapacitors containing chitin-bound electrodes and 1 M  $\text{Li}_2\text{SO}_4$  aqueous electrolyte (a), 1 M  $\text{Et}_4\text{NBF}_4$  organic electrolyte (b),  $[\text{EMIm}][\text{BF}_4]$ -based electrolyte (c), or  $[\text{MPPyrr}][\text{TFSI}]$ -based electrolyte (d) measured by galvanostatic charge and discharge technique. The results of GCD measurements at  $1 \text{ A g}^{-1}$  current density were presented in 2- and 3-electrode systems.

Table 3

The summary of specific capacitance values calculated from CV and GCD measurements for capacitor systems containing chitin- and PVdF-bound electrodes.

Electrolyte	Capacitance/ $\text{F g}^{-1}$			
	chitin-based binder		PVdF-based binder	
	<sup>a</sup> CV	<sup>b</sup> GCD	<sup>a</sup> CV	<sup>b</sup> GCD
1 M $\text{Li}_2\text{SO}_4$ in $\text{H}_2\text{O}$	128	128	115	117
1 M $\text{TEABF}_4$ in PC	141	140	121	121
$\text{EMImBF}_4$	142	142	125	123
$\text{MPPyrrTFSI}$	140	140	123	119

<sup>a</sup> From measurements at  $10 \text{ mV s}^{-1}$

<sup>b</sup> From measurements at  $1 \text{ A g}^{-1}$

measurements performed on PVdF-based electrodes are presented in Fig. S6. As can be seen, the reference system assembled with MPPyrrTFSI electrolyte showed almost the same performance as the chitin-based one, but the rest supercapacitors displayed lower capacitance retention efficiency.

One of the most important features of a supercapacitor is its long-term cyclic stability. To study this aspect, constant current cycling measurements at  $1 \text{ A g}^{-1}$  have been applied for all investigated devices (Fig. 8c). Upon 10,000 cycles, the electrochemical efficiency of chitin-bound electrodes applied in all the tested capacitors provides excellent capacitance retention. The system with aqueous electrolyte almost completely (*ca.* 99% capacitance retention) remains its starting capacitance over thousands of GCD cycles and the rest devices provide at least 75% of the initial capacitance at the end of this measurement. It suggests, coupled with all previously presented research results, that the chitin-bound electrode material is an eco-friendly, efficient, and high electrochemically stable alternative for traditional, synthetic polymer-bound carbon electrodes.

The PVdF-bound electrodes showed significantly lower long-term cyclic stability compared to the proposed chitin-bound electrodes (Fig. S7). Besides the most efficient system with MPPyrrTFSI electrolyte, other tested devices were dramatically losing initial capacitance value during GCD cycles. It confirms our observations from previously

performed measurements, indicating poor compatibility of PVdF binder with applied carbon cloth current collector. It should be noted, however, that the PVdF-bound electrode was prepared in an analogical way like the chitin-bound one, changing only the type of solvent. No improvement efforts in the synthesis method have been made. Thus, a hasty conclusion about the generally low performance of PVdF-bound electrodes should be avoided. It is widely known that PVdF works efficiently as an electrode binder on the surface of metallic current collectors, but it has failed as a binder on the microporous layer of woven carbon cloth. More information about the performance of PVdF-bound electrodes could be found in a recent review paper focused on the application of PVdF in supercapacitors [43]. Nevertheless, apart from the discussion about PVdF performance, this research has highlighted that chitin exhibits high compatibility with the carbon-based current collector, providing excellent adhesion of the electrode constitutes and an outstanding electrochemical efficiency with the eco-sustainable and biocompatible attribute.

To summarise our discussion, the power-energy density characteristic of systems based on chitin-bound electrode materials and various investigated electrolytes has been presented on the so-called Ragone plot (Fig. 8d). Supercapacitors, fundamentally, stand out as high power density devices. Thus, there is no difference in the case of the investigated systems. They display power density values even above  $10,000 \text{ W kg}^{-1}$  within the applied current density range. However, more interesting is the energy density performance of those devices. It is clearly visible, that maximum working voltage significantly influences the energy of a supercapacitor. So, the capacitors based on investigated chitin-bound electrode material reveal different energy densities, depending on the applied electrolyte. They show *ca.* 3, 35, 45, or  $60 \text{ Wh kg}^{-1}$  in a wide power density range, in the case of aqueous ( $\text{Li}_2\text{SO}_4$ ), organic ( $\text{Et}_4\text{NBF}_4$ ), or neat  $\text{EMIMBF}_4$  and  $\text{MPPyrrTFSI}$  electrolyte, respectively. Those values indicate the very efficient performance of investigated devices, thus, the chitin-bound electrode material seems to be a competitive alternative for already spread electrode constructions [44].

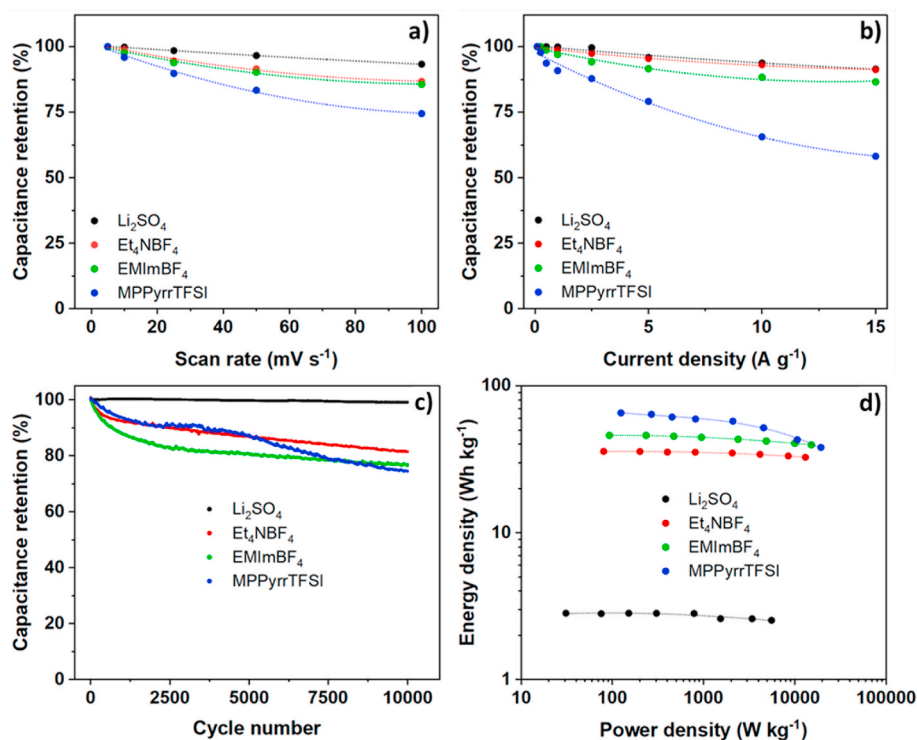


Fig. 8. Capacitance retention calculated from CV (a) and GCD (b) measurements, long-term cycling stability at a current density of  $1 \text{ A g}^{-1}$  (c) and Ragone plot (d) of supercapacitors assembled with chitin-bound electrodes and various liquid electrolytes.

#### 4. Conclusion

It has been reported that chitin is a promising, universal, and eco-friendly binder for carbonaceous-based electrode materials dedicated to supercapacitors. The investigated material can successfully replace commonly used synthetic polymers, such as fluorinated polymers PTFE or PVdF, while additionally presenting high performance in terms of electrochemical properties and long-term stability. Moreover, the proposed chitin-bound preparation procedure reduces the necessity of harsh solvent usage. The described method applied non-volatile ionic liquid recognized as *green solvent* and DMSO which is placed in the safest category of solvents.

Importantly, the designed chitin-bound electrode material exhibits outstanding electrochemical performance combined with versatility in terms of electrolyte compatibility. For the first time, we have proved that activated carbon-chitin composites can effectively operate with all typical types of liquid electrolytes dedicated to supercapacitors, i.e. aqueous-, organic-, and ionic liquid-based systems. Contrary to aqueous soluble biopolymer binders that are limited to application with organic- and ionic liquid-based electrolytes, chitin becoming a more universal choice.

The eco-friendly character of the chitin and sustainable nature of the preparation process of chitin-bound electrodes opens the doors for developing more *green* components for electrochemical capacitors. The recent achievement on chitin-bound electrodes, combined with our previous studies on chitin materials, brings us closer to the realization of an idea of fully sustainable components-based electrochemical capacitors.

#### CRedit authorship contribution statement

**Dawid Kasprzak:** Conceptualization, Methodology, Writing – original draft, Data curation. **Maciej Galiński:** Supervision, Writing – review & editing.

#### Declaration of competing interest

The authors declare the following financial interests/personal relationships which may be considered as potential competing interests: Dawid Kasprzak reports financial support was provided by Polish National Science Centre.

#### Data availability

Data will be made available on request.

#### Acknowledgment

This work was performed with the financial support of National Science Centre, Poland (grant no. 2019/33/N/ST5/01598).

#### Appendix A. Supplementary data

Supplementary data to this article can be found online at <https://doi.org/10.1016/j.jpowsour.2022.232300>.

#### References

- [1] H. Ibrahim, A. Ilinca, J. Perron, Energy storage systems-Characteristics and comparisons, *Renew. Sustain. Energy Rev.* 12 (2008) 1221–1250, <https://doi.org/10.1016/j.rser.2007.01.023>.
- [2] N.L. Panwar, S.C. Kaushik, S. Kothari, Role of renewable energy sources in environmental protection: a review, *Renew. Sustain. Energy Rev.* 15 (2011) 1513–1524, <https://doi.org/10.1016/j.rser.2010.11.037>.
- [3] O. Ellabban, H. Abu-Rub, F. Blaabjerg, Renewable energy resources: current status, future prospects and their enabling technology, *Renew. Sustain. Energy Rev.* 39 (2014) 748–764, <https://doi.org/10.1016/j.rser.2014.07.113>.
- [4] J.M. Tarascon, M. Armand, Issues and challenges facing rechargeable lithium batteries, *Nature* 414 (2001) 359–367, <https://doi.org/10.1038/35104644>.
- [5] B.C.H. Steele, A. Heinzel, Materials for fuel-cell technologies, *Nature* 414 (2001) 345–352, <https://doi.org/10.1038/35104620>.
- [6] A. Manthiram, Y. Fu, S. Chung, C. Zu, Y. Su, Rechargeable lithium – sulfur batteries, *Chem. Rev.* 114 (2014) 11751–11787.

- [7] Y. Wang, Y. Song, Y. Xia, Electrochemical capacitors: mechanism, materials, systems, characterization and applications, *Chem. Soc. Rev.* 45 (2016) 5925–5950, <https://doi.org/10.1039/c5cs00580a>.
- [8] J.Y. Hwang, S.T. Myung, Y.K. Sun, Sodium-ion batteries: present and future, *Chem. Soc. Rev.* 46 (2017) 3529–3614, <https://doi.org/10.1039/c6cs00776g>.
- [9] P. Pórolniczak, M. Walkowiak, J. Kaźmierczak-Rażna, D. Kasprzak, D.E. Mathew, M. Kathiresan, A.M. Stephan, N. Angulakshmi, BaTiO<sub>3</sub>-G-GO as an efficient permselective material for lithium-sulfur batteries, *Mater. Chem. Front.* 5 (2021) 950–960, <https://doi.org/10.1039/d0qm00716a>.
- [10] L. Liu, N. Solin, O. Inganäs, Bio based batteries, *Adv. Energy Mater.* 11 (2021) 1–12, <https://doi.org/10.1002/aem.202003713>.
- [11] S. Lin, F. Wang, Z. Shao, Biomass applied in supercapacitor energy storage devices, *J. Mater. Sci.* 56 (2021) 1943–1979, <https://doi.org/10.1007/s10853-020-05356-1>.
- [12] K. Fic, A. Platek, J. Piwek, E. Frackowiak, Sustainable materials for electrochemical capacitors, *Mater. Today* 21 (2018) 437–454, <https://doi.org/10.1016/j.matmod.2018.03.005>.
- [13] Q. Gao, L. Demarconnay, E. Raymundo-Piñero, F. Béguin, Exploring the large voltage range of carbon/carbon supercapacitors in aqueous lithium sulfate electrolyte, *Energy Environ. Sci.* 5 (2012) 9611–9617, <https://doi.org/10.1039/c2ee22284a>.
- [14] B. Gorska, E. Frackowiak, F. Béguin, Redox active electrolytes in carbon/carbon electrochemical capacitors, *Curr. Opin. Electrochem.* 9 (2018) 95–105, <https://doi.org/10.1016/j.coelec.2018.05.006>.
- [15] S. Saini, P. Chand, A. Joshi, Biomass derived carbon for supercapacitor applications: Review, *J. Energy Storage* 39 (2021), 102646, <https://doi.org/10.1016/j.est.2021.102646>.
- [16] D. Kasprzak, M. Galiński, Chitin and chitin-cellulose composite hydrogels prepared by ionic liquid-based process as the novel electrolytes for electrochemical capacitors, *J. Solid State Electrochem.* 25 (2021) 2549–2563, <https://doi.org/10.1007/s10008-021-05036-3>.
- [17] I. Stepniak, M. Galiński, K. Nowacki, M. Wysokowski, P. Jakubowska, V. V. Bazhenov, T. Leisegang, H. Ehrlich, T. Jesionowski, A novel chitosan/sponge chitin origin material as a membrane for supercapacitors – preparation and characterization, *RSC Adv.* 6 (2016) 4007–4013, <https://doi.org/10.1039/CSRA22047E>.
- [18] M. Wysokowski, K. Nowacki, F. Jaworski, M. Niemczak, P. Bartzczak, M. Sandomierski, A. Piasecki, M. Galiński, T. Jesionowski, Ionic liquid-assisted synthesis of chitin–ethylene glycol hydrogels as electrolyte membranes for sustainable electrochemical capacitors, *Sci. Rep.* 12 (2022) 1–15, <https://doi.org/10.1038/s41598-022-12931-w>.
- [19] D. Kasprzak, M. Galiński, Biopolymer-based gel electrolytes with an ionic liquid for high-voltage electrochemical capacitors, *Electrochem. Commun.* 138 (2022), 107282, <https://doi.org/10.1016/j.elecom.2022.107282>.
- [20] Z. Zhu, S. Tang, J. Yuan, X. Qin, Y. Deng, R. Qu, G.M. Haarberg, Effects of various binders on supercapacitor performances, *Int. J. Electrochem. Sci.* 11 (2016) 8270–8279, <https://doi.org/10.20964/2016.10.04>.
- [21] B. Dyatkin, V. Presser, M. Heon, M.R. Lukatskaya, M. Beidaghi, Y. Gogotsi, Development of a green supercapacitor composed entirely of environmentally friendly materials, *ChemSusChem* 6 (2013) 2269–2280, <https://doi.org/10.1002/cssc.201300852>.
- [22] M. Aslan, D. Weingarth, N. Jäckel, J.S. Atchison, I. Grobelsek, V. Presser, Polyvinylpyrrolidone as binder for castable supercapacitor electrodes with high electrochemical performance in organic electrolytes, *J. Power Sources* 266 (2014) 374–383, <https://doi.org/10.1016/j.jpowsour.2014.05.031>.
- [23] M. Aslan, D. Weingarth, P. Herbeck-Engel, I. Grobelsek, V. Presser, Polyvinylpyrrolidone/polyvinyl butyral composite as a stable binder for castable supercapacitor electrodes in aqueous electrolytes, *J. Power Sources* 279 (2015) 323–333, <https://doi.org/10.1016/j.jpowsour.2014.12.151>.
- [24] V. Khomenko, V. Barsukov, O. Chernysh, I. Makyeyeva, S. Isikli, F. Gauthy, Green Alternative binders for high-voltage electrochemical capacitors, *IOP Conf. Ser. Mater. Sci. Eng.* 111 (2016), 012025, <https://doi.org/10.1088/1757-899X/111/1/012025>.
- [25] A. Varzi, A. Balducci, S. Passerini, Natural cellulose: a green alternative binder for high voltage electrochemical double layer capacitors containing ionic liquid-based electrolytes, *J. Electrochem. Soc.* 161 (2014) A368–A375, <https://doi.org/10.1149/2.063403jes>.
- [26] D. Kasprzak, I. Stepniak, M. Galiński, Electrodes and hydrogel electrolytes based on cellulose: fabrication and characterization as EDLC components, *J. Solid State Electrochem.* 22 (2018) 3035–3047, <https://doi.org/10.1007/s10008-018-4015-y>.
- [27] J.H. Choi, Y. Kim, B. su Kim, Multifunctional role of reduced graphene oxide binder for high performance supercapacitor with commercial-level mass loading, *J. Power Sources* 454 (2020), 227917, <https://doi.org/10.1016/j.jpowsour.2020.227917>.
- [28] A. Kolodziej, K. Fic, E. Frackowiak, Towards sustainable power sources: chitin-bound carbon electrodes for electrochemical capacitors, *J. Mater. Chem. A* 3 (2015) 22923–22930, <https://doi.org/10.1039/c5ta06750b>.
- [29] P.K. Dutta, J. Duta, V.S. Tripathi, Chitin and chitosan: Chemistry, properties and applications, *J. Sci. Ind. Res. (India)* 63 (2004) 20–31, <https://doi.org/10.1002/chin.200727270>.
- [30] H. Ehrlich, P.G. Koutsoukos, K.D. Demadis, O.S. Pokrovsky, Principles of demineralization: modern strategies for the isolation of organic frameworks. Part I. Common definitions and history, *Micron* 39 (2008) 1062–1091, <https://doi.org/10.1016/j.micron.2008.02.004>.
- [31] D. Klemm, B. Heublein, H.P. Fink, A. Bohn, Cellulose: fascinating biopolymer and sustainable raw material, *Angew. Chem. Int. Ed.* 44 (2005) 3358–3393, <https://doi.org/10.1002/anie.200460587>.
- [32] M. Rinaudo, Chitin and chitosan: properties and applications, *Prog. Polym. Sci.* 31 (2006) 603–632, <https://doi.org/10.1016/j.procpolymsci.2006.06.001>.
- [33] M.V. Tsurkan, A. Voronkina, Y. Khrunyk, M. Wysokowski, I. Petrenko, H. Ehrlich, Progress in chitin analytics, *Carbohydr. Polym.* 252 (2021), 117204, <https://doi.org/10.1016/j.carbpol.2020.117204>.
- [34] J. ichi Kadokawa, Dissolution, derivatization, and functionalization of chitin in ionic liquid, *Int. J. Biol. Macromol.* 123 (2019) 732–737, <https://doi.org/10.1016/j.jbiomac.2018.11.165>.
- [35] J.L. Shamshina, Chitin in ionic liquids: historical insights into the polymer’s dissolution and isolation. A review, *Green Chem.* 21 (2019) 3974–3993, <https://doi.org/10.1039/c9gc01830a>.
- [36] Y. Zhong, J. Cai, L.N. Zhang, A review of chitin solvents and their dissolution mechanisms, *Chin. J. Polym. Sci.* 38 (2020) 1047–1060, <https://doi.org/10.1007/s10118-020-2459-x>.
- [37] M.M. Jaworska, I. Stepniak, M. Galiński, D. Kasprzak, D. Biniś, A. Górak, Modification of chitin structure with tailored ionic liquids, *Carbohydr. Polym.* 202 (2018) 397–403, <https://doi.org/10.1016/j.carbpol.2018.09.012>.
- [38] D. Kasprzak, M. Galiński, DMSO as an auxiliary solvent in the fabrication of homogeneous chitin-based films obtaining from an ionic liquid process, *Eur. Polym. J.* 158 (2021), 110681, <https://doi.org/10.1016/j.eurpolymj.2021.110681>.
- [39] M. Thommes, K. Kaneko, A.V. Neimark, J.P. Olivier, F. Rodriguez-Reinoso, J. Rouquerol, K.S.W. Sing, Physisorption of gases, with special reference to the evaluation of surface area and pore size distribution (IUPAC Technical Report), *Pure Appl. Chem.* 87 (2015) 1051–1069, <https://doi.org/10.1515/pac-2014-1117>.
- [40] E. Frackowiak, Carbon materials for supercapacitor application, *Phys. Chem. Chem. Phys.* 9 (2007) 1774–1785, <https://doi.org/10.1039/b618139m>.
- [41] H.Y. Hu, N. Xie, C. Wang, F. Wu, M. Pan, H.F. Li, P. Wu, X. Di Wang, Z. Zeng, S. Deng, M.H. Wu, K. Vinodgopal, G.P. Dai, Enhancing the performance of motive power lead-acid batteries by high surface area carbon black additives, *Appl. Sci.* 9 (2019), <https://doi.org/10.3390/app9010186>.
- [42] Z. Xiao, W. Chen, K. Liu, P. Cui, D. Zhan, Porous biomass carbon derived from peanut shells as electrode materials with enhanced electrochemical performance for supercapacitors, *Int. J. Electrochem. Sci.* 13 (2018) 5370–5381, <https://doi.org/10.20964/2018.06.54>.
- [43] S. Rajeevan, S. John, S.C. George, Polyvinylidene fluoride: a multifunctional polymer in supercapacitor applications, *J. Power Sources* 504 (2021), 230037, <https://doi.org/10.1016/j.jpowsour.2021.230037>.
- [44] P. Simon, Y. Gogotsi, Materials for electrochemical capacitors, *Nat. Mater.* 7 (2008) 845–854, <https://doi.org/10.1038/nmat2297>.